Solid-State Solvation and Enhanced Exciton Diffusion in Doped Organic Thin Films under Mechanical Pressure

Wendi Chang,[†] Gleb M. Akselrod,[‡] and Vladimir Bulović*[,†]

[†]Department of Electrical Engineering and Computer Science, Massachusetts Institute of Technology, Cambridge, Massachusetts 02139, United States and
[‡]Department of Electrical and Computer Engineering Duke, University, Durham, North Carolina 27708, United States

ABSTRACT Direct modification of exciton energy has been previously used to optimize the operation of organic optoelectronic devices. One demonstrated method for exciton energy modification is through the use of the solvent dielectric effects in doped molecular films. To gain a deeper appreciation of the underlying physical mechanisms, in this work we test the solid-state solvation effect in molecular thin films under applied external pressure. We observe that external mechanical pressure increases dipole−dipole interactions, leading to shifts in the Frenkel exciton energy and enhancement of the time-resolved spectral red shift associated with the energy-transfer-mediated exciton diffusion. Measurements are performed on host:dopant molecular thin films, which show bathochromic shifts in photoluminescence (PL) under increasing pressure. This is in agreement with a simple solvation theory model of exciton energetics with a fitting parameter based on the mechanical properties of the host matrix material. We measure no significant change in exciton lifetime with increasing pressure, consistent with unchanged aggregation in molecular films under compression. However, we do observe an increase in exciton spectral thermalization rate for compressed molecular films, indicating enhanced exciton diffusion for increased dipole−dipole interactions under pressure. The results highlight the contrast between molecular energy landscapes obtained when dipole−dipole interactions are increased by the pressure technique *versus* the conventional dopant concentration variation methods, which can lead to extraneous effects such as aggregation at higher doping concentrations. The present work demonstrates the use of pressure-probing techniques in studying energy disorder and exciton dynamics in amorphous molecular thin films.

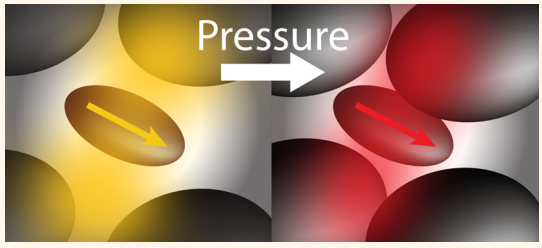

KEYWORDS: organic semiconductor · solid-state solvation effect · Onsager dielectric theory · pressure probing · Förster radiative energy transfer

Organic semiconductors have been used in a variety of applications including photodetectors,[1] xerographic photoreceptors,[2] LED pixels in displays,[3,4] solid-state lighting elements,[5] thin film photovoltaics,[6] and chemosensors.[7] In many examples of these technologies, host:dopant molecular thin films are employed. Since the solid-state molecular thin films are van der Waals bonded, dipole−dipole interactions between the host and dopant can strongly affect the energy level structure of constituent molecules, leading to the solvation effect.[8−11] This effect can be particularly pronounced in blended molecular thin films.

The solvation effect is an electrostatic phenomenon caused by dipolar interaction between a solute (dopant) molecule and solvent (host matrix) molecules upon photoexcitation or emission. This interaction simultaneously affects both excitonic ground and excited states of the solute molecules, modifying both the absorption and emission spectra. As polarizability of the solvent increases, the reaction electric field from solvent reorientation during absorption and emission of the solute also increases. For solute molecules with a large transition dipole moment, this solvation effect typically results in a bathochromic (red) shift in the transition energy in more polarizable solvent (Figure 1b). The solvation effect has been extensively studied through photoluminescence (PL) measurements in the liquid state, with molecular luminophores dissolved in solvents of different polarizability.[8,9] These studies were followed by reports of solvation in doped molecular thin films, a phenomenon which has been termed the solid-state solvation effect (SSSE), as it exhibits the same quantifiable behavior as the liquid-state solvation effect.[10−13]

* Address correspondence to bulovic@mit.edu.

Received for review February 9, 2015 and accepted April 2, 2015.

Published online April 02, 2015
10.1021/acsnano.5b00938

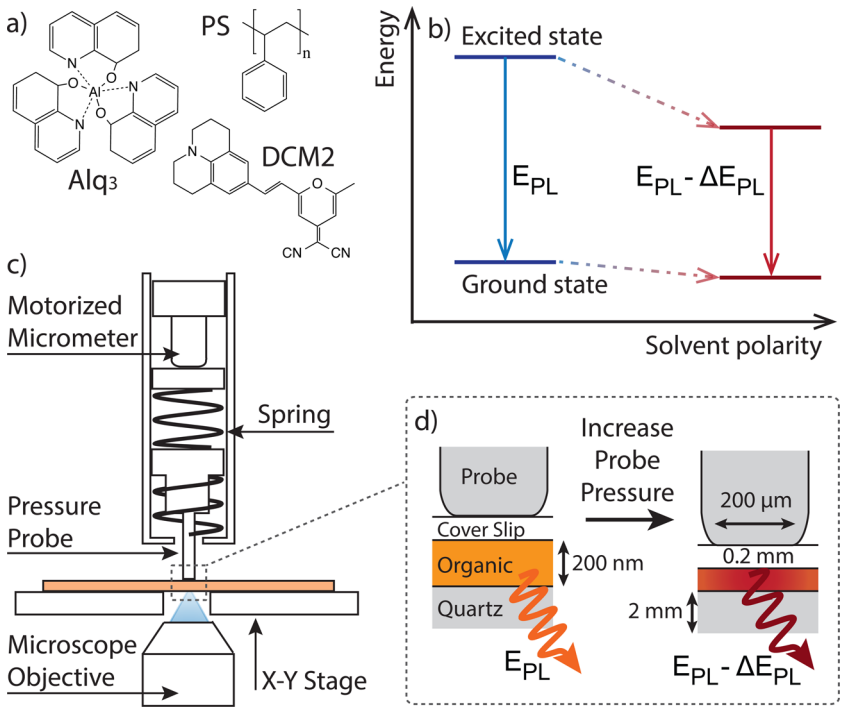

Figure 1. (a) Chemical structure of DCM2 dopant molecules and PS polymer dielectric matrix and Alq_3 molecular matrix. (b) Schematic of SSSE on energy levels, illustrating bathochromic (red) shift in the PL peak for typical dye molecules due to increasing dielectric matrix polarity; increase in the matrix polarity causes a larger reaction field in response to the optical-excitation of dopant molecules and subsequent emission, creating a larger perturbation on the energy levels to red shift the transition energy. (c) Experimental setup for in situ optical measurement of an organic thin film sample under mechanical pressure. The motorized micrometer and spring in series apply a linearized displacement force on the film. The $x-y$ stage supports the pressure setup and moves relative to the excitation spot. The microscope objective both focuses an excitation laser onto the film and captures subsequent exciton emission. (d) Illustration of change in PL energy, ΔE_{PL}, under increased mechanical pressure applied to the sample.

Previous work on SSSE demonstrated tuning of the emission wavelength of polar luminescent dopant molecules by varying their concentration in a nonemissive host matrix.[10] This study reported up to 75 nm tuning of the peak emission wavelength through doping of the laser dye 4-(dicyanomethylene)-2-methyl-6-(julolidin-4-ylvinyl)-4*H*-pyran) (DCM2) in tris(8-hydroxyquinoline)aluminum (Alq_3) (Figure 1a) or *N*,*N*-diphenyl-*N*,*N*-bis(3-methylphenyl)-1,1-biphenyl-4,4-diamine (TPD) host films.[10] In addition to the dopant concentration, additional factors such as aggregation of the dopant molecules in host films could also manifest and contribute to the observed red shift in energy. Indeed, the efficiency of the PL process typically decreases at higher dopant concentrations, as would be expected from aggregated luminophores. Attempting to isolate the SSSE from luminophore aggregation, another study examined the effect of varying the concentration of a polar nonemissive co-dopant in a nonpolar host matrix while keeping the dopant molecule concentration constant: a 40 nm wavelength shift in peak PL was reported for a series of samples with 0.005% doping of DCM2 molecules in a polystyrene (PS) matrix by varying the doping levels of polar camphoric anhydride (CA) co-dopant molecules, which affected the average dielectric response of the matrix.[11] In addition, the liquid-state Onsager[14] model and Ooshika–Lippert–Mataga (OLM) solvation theory[15–18] were applied to solid-state measurements to show good agreement for co-doping experiments.[11] However, due to the complexity of a three-material co-doped system and possible errors introduced in sample-to-sample variation, it is desirable to develop an alternative method for examining interactions at the molecular level, which we present in this study.

We employ a mechanical pressure probing technique to demonstrate PL spectral tuning through pressure-enhanced SSSE in optically excited molecular thin film samples. Previous studies utilized pressure techniques to observe changes in the exciplex charge-transfer state between donor and acceptor molecules[19,20] and even deformation of polymer and large dye molecules.[21,22] In our work, mechanical pressure affects the density of molecules in the film, which in turn modifies the local dielectric effects and manifests in enhanced SSSE (see Figure 1).

RESULTS

Externally applied mechanical pressure can cause film deformation, decreasing the intermolecular distance, leading to increasing solvent polarity (Figure 1). This effectively modifies the local dielectric matrix

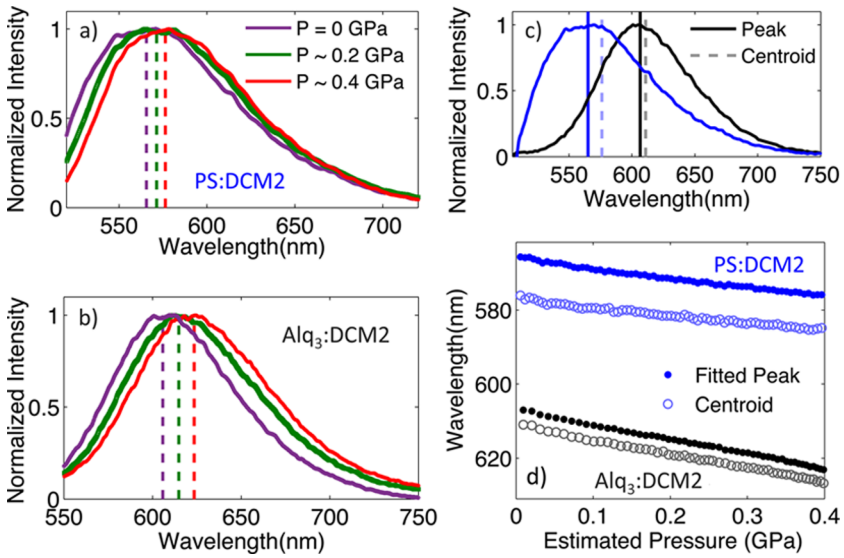

Figure 2. Spectral shift in PL of the (a) film of 0.5% doped DCM2 in PS, (b) film of 1% doped DCM2 in Alq_3, in response to the externally applied pressure (with estimated pressure, indicated in the legend). The peak wavelength, as determined from numerically fitting the PL, is indicated for each spectrum with a vertical dashed line. (c) Plot of PL spectra of PS:DCM2 and Alq_3:DCM2 films under no pressure and the corresponding peak (solid line) and centroid (dashed line) of each spectrum. The peaks are computed from a Gaussian fit of each PL spectrum, with errors within 1 nm. The centroid is computed from a weighted averaging of intensity counts at each wavelength for PL above the half-maximum point. (d) Spectral shift of the PL peak wavelength and centroid as a function of applied pressure for 0.5% doping of DCM2 in PS (top) and 1% doping of DCM2 in Alq_3 (bottom).

environment using a controlled external parameter. Since increasing the molecular density increases the matrix polarity, we expect a bathochromic (red) shift in the PL for DCM2 dopant molecules, similar to previously reported results for films of increased doping concentration.[10,11] In this work, measurements are performed on low-doped (≤1% by weight) organic thin films of Alq_3:DCM2 and PS:DCM2 (Figure 1) under varying amounts of external pressure, and results are compared with traditional doping concentration experiments.

Parts a and b of Figure 2 show the measured PL spectrum of the corresponding sample under select pressures, with dashed lines indicating fitted peak wavelengths. Under increasing pressure, a reversible bathochromic shift in the peak PL wavelength is observed: over $\Delta\lambda$ = 10 nm for samples of PS:DCM2 and over $\Delta\lambda$ = 15 nm for Alq_3:DCM2 samples, as the estimated applied pressure changes from 0 to 0.4 GPa. Figure 2d compares fitted peaks and computed centroids for the two measured material systems. For both systems, the PL spectrum under pressure shows negligible changes in emission line width, and shifts in PL centroids are well correlated with the shifts in peak PL wavelength, confirming the homogeneity of the spectral shift among the measured dye molecules. These observed effects on PL emission are consistent with the expected increase in the local dielectric constant due to increase in density of dopant and host molecules.

To compare the measured data to the expected change due to SSSE, we use a dielectric continuum model with standard assumptions consistent with the Onsager model,[14] namely that the solute (dopant) electronic densities are reduced to dipoles and the solute molecules are enclosed in spherical cavities and are only affected by neighboring molecules within a certain constant radius a. In the Stark perturbation consideration, a change in the transition energy as measured by emission according to OLM solvation theory is expressed as[15−18]

$$\Delta E_{PL} = -\frac{\Delta\vec{\mu}}{a^3}(\Lambda(\epsilon)\vec{\mu}_e + \Lambda(n^2)\vec{\mu}_g)$$

where

$$\Lambda(x) = \frac{2(x-1)}{2x+1} \quad (1)$$

The high frequency solvent electron reorientation term $\Lambda(n^2)$ with index of refraction n is approximated to be on the same time scale with solute absorption and emission. Its contribution is assumed to be relatively invariant as a function of solvent (matrix) polarizability compared to the low-frequency solvent nuclear reorientation term $\Lambda(\epsilon)$, with ϵ as the solvent dielectric constant. We assume that the dipole moments of the excited state $\vec{\mu}_e$, the ground state $\vec{\mu}_g$, and the transition dipole $\Delta\vec{\mu} = \vec{\mu}_g - \vec{\mu}_e$ are only dependent on the solute molecule and are also constant with pressure. These assumptions result in a simple relationship between the change in transition energy and the local dielectric constant

$$\Delta E_{PL} \approx -A\Lambda(\epsilon) + C \quad (2)$$

with parameter values A = 0.55 eV and C = 2.4 eV taken from the literature, where they were shown to

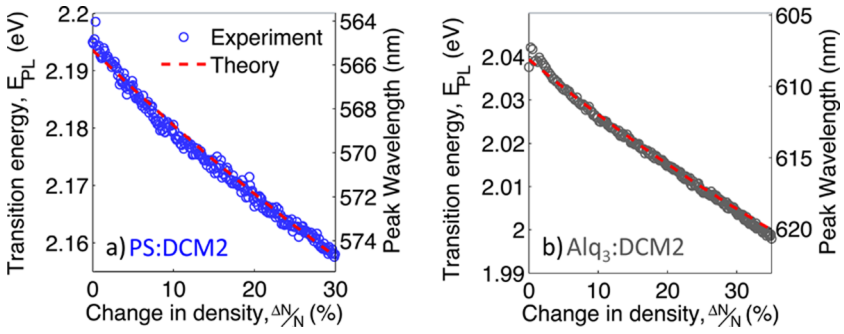

Figure 3. Fitting experimental results of peak PL energy shift of (a) PS:DCM2 and (b) Alq_3:DCM2 films as a function of change in the molecular packing density or equivalent change in dielectric susceptibility. The red dashed lines indicate predicted OLM theory, and circles indicate the experimentally observed peak PL wavelength shift converted to change in density using fitting parameter α.

correspond to DCM2 in both the liquid and solid states.[11] Assuming proportionality between dielectric susceptibility χ and the density of surrounding matrix molecules N, $\chi = \epsilon - 1 \propto N$, we have a direct relationship between change in ϵ and the volumetric change of the material. The volumetric change can be directly related to uniaxial pressure, P, through Poisson's ratio ν and Young's modulus Y of the host material:

$$\frac{\Delta\epsilon}{\epsilon - 1} = \frac{\Delta N}{N} = \left|\frac{\Delta V}{V_0}\right| = \left|\left(1+\frac{P}{Y}\right)^{1-2\nu} - 1\right| \quad (3)$$

To further simplify our fit, we can approximate the relationship using the first term of the Taylor expansion about zero pressure, resulting in a linear relationship between external pressure and volumetric change with proportionality constant α.

$$\frac{\Delta\epsilon}{\epsilon - 1} \approx \frac{1-2\nu}{Y} P = \alpha P \quad (4)$$

Substituting eq 4 into eq 2 we obtain a model describing the expected change of the PL energy under uniaxial pressure, using α as a single fitting parameter. In Figure 3, the PS:DCM2 experimental results are compared to this simplified OLM theory, using $\alpha_{PS} = 0.8 \pm 0.4\ GPa^{-1}$, showing a good agreement. We can also calculate α_{PS} by using the literature values of the PS Poisson ratio,[23] $\nu = 0.35$, and Young's modulus,[24] $Y = 1.3$ GPa, to find an expected value of $\alpha_{PS} = 0.23\ GPa^{-1}$. Accounting for the error in the fit, the calculated and fit-to-experiment values of α_{PS} are within a factor of 2. Such discrepancy could be due to the simplifying assumptions made in the above theory development or due to the differences in ν and Y of our doped PS films, as compared to the neat films measured in the literature.

The same fit to theory can be performed for the Alq_3:DCM2 films, shown in Figure 3b, resulting in $\alpha_{Alq3} = 1.1 \pm 0.5\ GPa^{-1}$. Literature estimates for the elastic modulus of Alq_3 vary widely, with a range of 1−100 GPa obtained by different methods such as wrinkle-based metrology measurements[25] and nanoindentation.[26] With more precise pressure tuning systems, our SSSE measurement and fitting technique may provide another method of estimating material properties. The simple steady-state PL measurement under external pressure demonstrates consistent measurement of solvation effect by observing the same illuminated spot on a single sample. This is in contrast to previous studies that necessitated multiple samples with different doping concentrations or material properties to obtain similar results.

To highlight the physical difference between density-dependent and doping-dependent SSSE, we use a

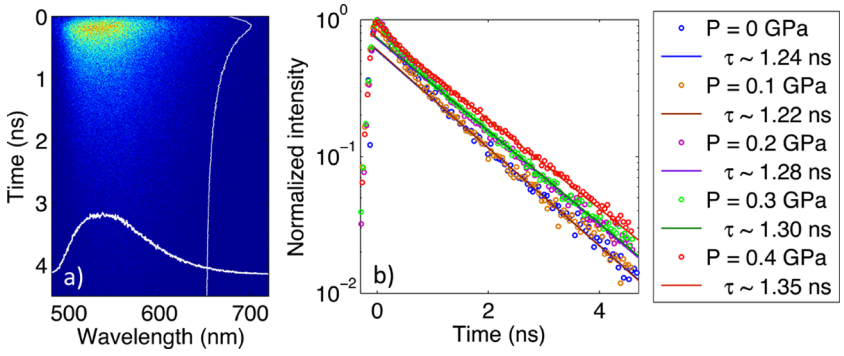

Figure 4. Streak camera PL measurement of PS:DCM2 film doped at 0.5%. (a) Spectrally integrated time-resolved emission plotted vertically on the right and time-integrated steady-state PL plotted horizontally on the bottom. (b) Time-resolved PL emission of PS:DCM2 integrated over all wavelengths for select pressures; corresponding lifetimes are listed in legend. The error in PL lifetime fits is ±0.05 ns.

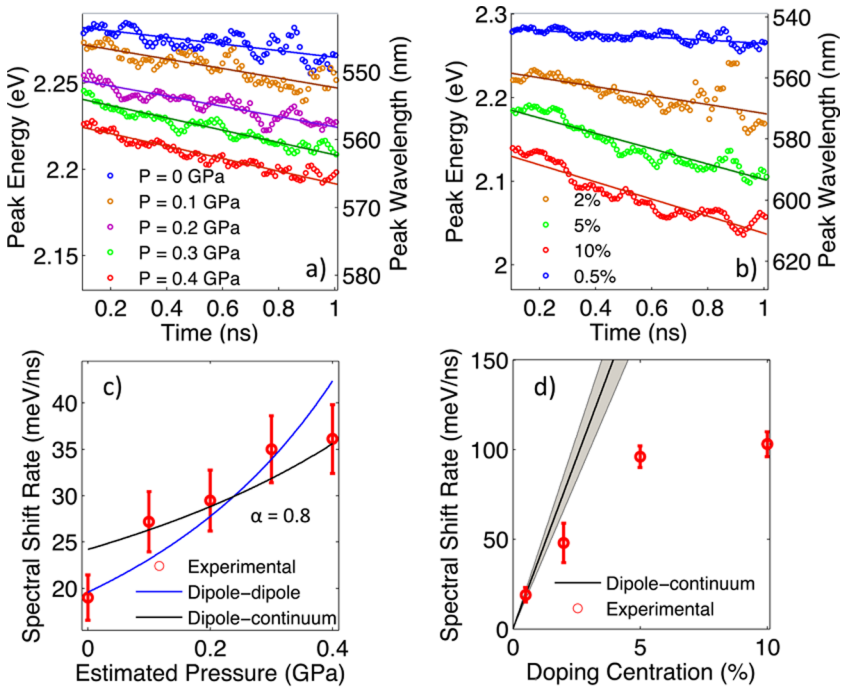

Figure 5. Spectral red-shift of peak PL emission of (a) films of PS:DCM2 at 0.5% doping for a range of applied pressures, showing increased exciton diffusion with increasing pressure; (b) films of PS:DCM2 at select dopings under zero pressure, showing similar trend in increasing spectral shift rate with increased doping concentration. The corresponding spectral shift rates are plotted in red for film (c) under select pressures and (d) select doping concentration. The solid lines correspond to the numerically determined spectral shift rate scale factor k/k_0, using both FRET models: dipole-to-single dipole interactions and dipole-to-dipole continuum interactions. The pressure effect in (c) is calculated based on solvation effect fitting parameter $\alpha = 0.8$ GPa. For various doping concentrations in (d), the large discrepancy between the dipole-to-dipole continuum model and experimental values at higher doping concentration highlights the necessity to consider additional variables in exciton energetics beyond density of dopant molecules.

streak camera to monitor the time-resolved exciton diffusion dynamics through observed spectral change over time. We measure samples of PS:DCM2 under different externally applied pressures, as well as samples with varying doping concentrations. The time-resolved data of a 0.5% doped thin film under select pressures is shown in Figure 4a. The corresponding fitted luminescence lifetimes are within 0.2 ns for the measured range of pressures. This is in contrast to previous time-resolved DCM doping PL studies,[27] where the lifetime significantly decreased with increased DCM concentration, due to the exciton quenching by aggregated dye molecules. This comparison highlights that the solvatochromic shift due to change in density in organic matrix under pressure does not exhibit the pronounced aggregation quenching effect on exciton lifetime.

Additionally, for each temporal slice of the spectral data in Figure 4a, the peak PL wavelength is computed. Evolution of the peak PL within the exciton lifetime (~1 ns) after initial excitation of 0.5% doped PS:DCM2 sample under different pressures is plotted in Figure 5a. The time-resolved spectral data shows a monotonic red-shift in PL with time, consistent with the previously observed exciton thermalization through the Förster-transfer-assisted exciton spatial diffusion.[28−30] This thermalization allows the exciton to Förster transfer from dopant to lower energy neighboring dopant molecules, which is manifested in the observed spectral red shift. Each set of spectral diffusion data is linearly fitted within the exciton lifetime, and the spectral shift rate corresponding to the slope of the fit is plotted in Figure 5c.

Since the observed red shift is due to excition thermalization dominated by Förster radiative energy transfer (FRET) between DCM2 molecules, we expect the rate of energy shift to increase due to increased matrix density for films under external applied pressure. We can model this effect in two limiting geometric cases: (1) dipole to single dipole interaction and (2) dipole to dipole continuum. To model the change in the spectral shift rate we assume a direct relationship between the spectral shift rate and the FRET rate.[31] Furthermore, we assume the Förster radius to be constant under the pressures applied. The FRET rate is given by the donor lifetime τ, the number of acceptor sites N_A, Förster radius R_{FRET}, and the DCM2−DCM2 molecular spacing, r:

$$k_{FRET} = \frac{N_A}{\tau}\frac{R_{FRET}^6}{r^6} \quad (4)$$

For the case of a single dipole−dipole interaction, we consider only the effect of change in r between

nearest neighbor DCM2 molecules (N_A = 1). The ensemble-averaged change in r is derived from the volumetric change due to uniaxial pressure, which in turn is obtained from the steady-state PL measurement. We use the fitting parameters from PS:DCM2 films to estimate the change in spectral shift rate, k, as a function of applied pressure, P:

$$\frac{k}{k_0} \approx \frac{r_0^6}{r^6} = \frac{1}{\left(1 - \frac{\Delta V}{V}\right)^2} = \frac{1}{(1 - \alpha P)^2} \quad (5)$$

For the case of dipole-to-dipole continuum interaction, the transfer rate is the integration, over all space, of each spherical shell of acceptor sites at radius r. Thus, the change in transfer rate under pressure does not follow the r^{-6} relationship but depends instead on the change in overall acceptor dipole density:

$$\frac{k}{k_0} \approx \frac{N_A}{N_{A,0}} = \frac{r_0^3}{r^3} = \frac{1}{1 - \alpha P} \quad (6)$$

In Figure 5c, using the steady-state fitted value of $\alpha = 0.8$ GPa, the two models are fitted to streak camera data within measurement errors, showing change in the spectral red-shift rate as a function of estimated pressure. The experimental data show an increase in the spectral shift rate with increasing pressure, which falls within the expected values based on FRET-mediated exciton transfer as represented by the two limiting cases. Therefore, the pressure-probing technique increases molecular dipole interactions, leading to enhanced exciton diffusion in organic thin films.

In contrast to the varying the acceptor density using pressure, we also vary the doping density of DCM2 in PS. Figure 5b shows the streak camera measurements of time-dependent peak PL for this series of PS:DCM2 samples, each with a different DCM2 doping concentration. A previous study found that the FRET rate at low doping concentrations follows more closely to a r^{-3} dependence rather than conventional dipole–dipole FRET r^{-6} dependence.[32] Thus, we use the density-dependent dipole-to-dipole continuum model described by eq 6; we assume that the spectral shift rate variation is only due to increased DCM2 acceptor molecules sites for higher concentration samples (see Figure 5d). Compared to the density-based prediction, the spectral shift rate still deviates significantly for higher doping concentrations. Clearly, more complex modeling is necessary to accurately describe measured rates when varying dopant concentration.[30,31] For such traditional doping techniques, molecular interactions can no longer be simply explained through increase of the number of neighboring dye molecules in the nonpolar solvent environment. Other factors such as dopant aggregation, increasing number of low energy transfer sites within Förster radius, and change in dopant dipole moments become significant variables. Thus, the presented pressure technique on thin films can be applied more generally to observation of spectral thermalization and excition diffusion with fewer complicating factors.

CONCLUSION

We demonstrate that the solid-state solvation effect observed in molecular thin films under pressure can be consistently predicted using a simplified model based on the change in the intermolecular distance with applied pressure. This technique allows for fine control of the exciton energy and could be implemented to study the effect of change of mechanical or electrostatic pressure on the excitons in optoelectronic molecular/polymeric devices. On the basis of solvation modeling and fit, the Förster-mediated spectral red-shift is consistent with the observed temporal and spectral-resolved PL measurements under pressure. Thus, the increase in spectral shift rate under pressure indicates enhanced exciton diffusion in organic thin films. Furthermore, comparison between pressure-induced change and doping concentration-induced change in this spectral shift rate show an advantage in using pressure to reduce the effects of additional variables such as aggregation. Such pressure probing technique could enable fundamental studies of electronic and excitonic energy disorder in molecular solids. Pressure systems to directly measure probe displacement could improve upon the technique for tuning exciton energy shifts and may provide additional benefits as an opto-mechanical method to estimate the material properties of molecular/polymeric host matrix films.

METHODS

Material Deposition. Two sets of material systems were prepared for this study: films of 200 nm thick Alq_3:DCM2 at 1% DCM2 doping were deposited on quartz substrates at a rate of 3.0 Å/s by using thermal coevaporation at a chamber pressure below 10^{-6} Torr. Films of 200 nm thick PS:DCM2 with 0.5% DCM2 doping were spin-cast from a 30 mg/mL chloroform solution at 2000 rpm.

Mechanical Setup. The mechanical pressure setup, shown in Figure 1c, includes force and sample position scanning capabilities as well as optical accessibility for PL measurement. A mechanical spring of spring constant 4.5 N/mm is inserted between the probe and the motorized micrometer for a linear force–displacement relationship, and pressure is estimated from force and contact area. Force is applied through a steel probe on an organic film sandwiched between a thick quartz substrate and a flexible cover glass, which is calibrated by using a load cell. The 200 μm contact diameter is estimated by imaging Newton interference rings between top cover glass and bottom quartz substrate. The measured diameter has a systematic error up to 20%, which contributes to uncertainty in the reported applied pressure.

Optical Characterization. Samples were excited using a 200 ps pulsed laser of $\lambda = 475$ nm focused to a spot diameter of 10 μm using a 5× Nikon objective. The steady-state PL was collected by the same objective and reimaged into a spectrograph (Princeton Instruments Acton SP2300) with a Si charge-coupled detector array (Princeton Instruments Pixis) to obtain emission spectra or steak camera (Hamamatsu) for time-resolved spectral data.

For each PL spectrum, the peak wavelength was found by using a peak Gaussian fit and the centroid was computed as a weighted average for all photon counts above half-maximum intensity point.

Conflict of Interest: The authors declare no competing financial interest.

Acknowledgment. This work is supported in part by the National Science Foundation and the US Department of Energy, Center for Excitonics, Award No. DE-SC0001088 (MIT), and made use of the shared facilities supported by the eni-MIT Solar Frontiers Center and managed by the MIT NSF Center for Material Science and Engineering. G.M.A. acknowledges support from the Hertz Foundation Fellowship and the National Science Foundation Graduate Research Fellowship.

REFERENCES AND NOTES

1. Peumans, P.; Bulović, V.; Forrest, S. R. Efficient, High-Bandwidth Organic Multilayer Photodetectors. *Appl. Phys. Lett.* **2000**, *76*, 3855.
2. Borsenberger, P. *Organic Photoreceptors for Xerography*; Marcel Dekker, Inc.: New York, 1998.
3. Tang, C. W.; VanSlyke, S. A. Organic Electroluminescent Diodes. *Appl. Phys. Lett.* **1987**, *51*, 913.
4. Tang, C. W.; VanSlyke, S. A.; Chen, C. H. Electroluminescence of Doped Organic Thin Films. *J. Appl. Phys.* **1989**, *65*, 3610.
5. D'Andrade, B. W.; Forrest, S. R. White Organic Light-Emitting Devices for Solid-State Lighting. *Adv. Mater.* **2004**, *16*, 1585–1595.
6. Tang, C. W. Two-Layer Organic Photovoltaic Cell. *Appl. Phys. Lett.* **1986**, *48*, 183.
7. Bernards, D.; Owens, R.; Malliaras, G. Solid-State Chemosensitive Organic Devices for Vapor-Phase Detection. *Organic Semiconductors in Sensor Applications*; Springer Series in Materials Science; Springer: New York, 2008; Vol. 107, pp 141−184.
8. Reichardt, C. *Solvents and Solvation Effects in Organic Chemistry*; VCH: New York, 1990.
9. Meyer, M.; Mialocq, J. C. Ground State and Singlet Excited State of Laser Dye DCM: Dipole Moments and Solvent Induced Spectral Shifts. *Opt. Commun.* **1987**, *64*, 264–268.
10. Bulovic, V.; Deshpande, R.; Thompson, M. E.; Forrest, S. R. Tuning the Color Emission of Thin Film Molecular Organic Light Emitting Devices by the Solid State Solvation Effect. *Chem. Phys. Lett.* **1999**, *308*, 317–322.
11. Madigan, C. F.; Bulović, V. Solid State Solvation in Amorphous Organic Thin Films. *Phys. Rev. Lett.* **2003**, *91*, 247403.
12. Bulović, V.; Baldo, M. A.; Forrest, S. R. Excitons and Energy Transfer in Doped Luminescent Molecular Organic Materials. In *Organic Electronic Materials: conjugated Polymers and Low Molecular Weight Organic Solids*; Farchioni, R., Grosso, G., Eds.; Springer: New York, 2001; pp 391−441.
13. Green, A. P.; Butler, K. T.; Buckley, A. R. Tuning of the Emission Energy of Fluorophores Using Solid State Solvation for Efficient Luminescent Solar Concentrators. *Appl. Phys. Lett.* **2013**, *102*, 133501.
14. Onsager, L. Electric Moments of Molecules in Liquids. *J. Am. Chem. Soc.* **1936**, *58*, 1486–1493.
15. Ooshika, Y. Absorption Spectra Of Dyes In Solution. *J. Phys. Soc. Jpn.* **1954**, *9*, 594.
16. Lippert, E. Dipolmoment und Elektronenstruktur von angeregten Molekülen. *Z. Naturforsch.* **1955**, *10A*, 541.
17. Mataga, N.; Kaifu, Y.; Koizumi, M. Solvent Effects upon Fluorescence Spectra and the Dipole Moments of Excited Molecules. *Bull. Chem. Soc. Jpn.* **1956**, *29*, 465.
18. Lakowicz, J. R. *Principles of Fluorescence Spectroscopy*, 3rd ed.; Springer: Singapore, 2006.
19. Schmidtke, J.; Friend, R.; Silva, C. Tuning Interfacial Charge-Transfer Excitons at Polymer-Polymer Heterojunctions under Hydrostatic Pressure. *Phys. Rev. Lett.* **2008**, *100*, 157401.
20. Chang, W.; Congreve, D. N.; Hontz, E.; Bahlke, M. E.; McMahon, D. P.; Reineke, S.; Wu, T. C.; Bulović, V.; Van Voorhis, T.; Baldo, M. Spin-Dependent Charge Transfer State Design Rules in Organic Photovoltaics. *Nat. Commun.* **2015**, *6*, 6415.
21. Chandrasekhar, M.; Guha, S.; Graupner, W. Squeezing Organic Conjugated Molecules − What Does One Learn? *Adv. Mater.* **2001**, *13*, 613–618.
22. Stöttinger, S.; Hinze, G.; Diezemann, G.; Oesterling, I.; Müllen, K.; Basché, T. Impact of Local Compressive Stress on the Optical Transitions of Single Organic Dye Molecules. *Nat. Nano.* **2014**, *9*, 182–186.
23. Brandrup, J.; Immergut, E. H.; Grulke, E. A. *Polymer Handbook*; Wiley: New York, 1999.
24. Torres, J. M.; Bakken, N.; Stafford, C. M.; Li, J.; Vogt, B. D. Thickness Dependence of the Elastic Modulus of Tris(8-hydroxyquinolinato)aluminium. *Soft Matter* **2010**, *6*, 5783.
25. Bakken, N.; Torres, J. M.; Li, J.; Vogt, B. D. Thickness Dependent Modulus of Vacuum Deposited Organic Molecular Glasses for Organic Electronics Applications. *Soft Matter* **2011**, *7*, 7269.
26. Chiang, C.-J.; Bull, S.; Winscom, C.; Monkman, A. A Nano-Indentation Study of the Reduced Elastic Modulus of Alq3 and NPB Thin-Film used in OLED Devices. *Org. Electron.* **2010**, *11*, 450–455.
27. Uddin, A.; Lee, C. B. Exciton Behaviours in Doped Tris(8-hydroxyquinoline)aluminum (Alq3) Films. *Phys. Status Solidi* **2011**, *8*, 80–83.
28. Förster, T. 10th Spiers Memorial Lecture. Transfer Mechanisms of Electronic Excitation. *Discuss. Faraday Soc.* **1959**, *27*, 7–17.
29. Madigan, C.; Bulović, V. Modeling of Exciton Diffusion in Amorphous Organic Thin Films. *Phys. Rev. Lett.* **2006**, *96*, No. 046404.
30. Fennel, F.; Lochbrunner, S. Förster-Mediated Spectral Diffusion in Disordered Organic Materials. *Phys. Rev. B* **2012**, *85*, No. 094203.
31. Eisenthal, K. B.; Siegel, S. Influence of Resonance Transfer on Luminescence Decay. *J. Chem. Phys.* **1964**, *41*, 652.
32. Green, A. P.; Buckley, A. R. Solid State Concentration Quenching of Organic Fluorophores in PMMA. *Phys. Chem. Chem. Phys.* **2015**, *17*, 1435–1440.